CHROMATIC EFFECTS IN QUADRUPOLE SCAN TECHNIQUE

E. Chiadroni_, M. Ferrario, D. Filippetto, INFN-LNF, Frascati, Italy
A. Cianchi, INFN and University of Rome "Tor Vergata", Rome, Italy
A. Mostacci, Dip. Energetica University of Rome "La Sapienza", Rome, Italy
C. Ronsivalle, ENEA C.R. Frascati, Italy

Abstract

A reliable transverse emittance measurement for highbrightness electron beams, in particular where the beam exhibits a significant energy spread, is of utmost importance for the successful development of the SPARC FEL. The effect of the emittance degradation induced by chromatic effects in the quadrupole scan measurement for different configurations of the magnetic lattice is evaluated. Analytical and numerical calculations compared with measurements are reported and discussed.

CHROMATIC EFFECTS IN QUADRUPOLE SCAN TECHNIQUE

E. Chiadroni*, M. Ferrario, D. Filippetto, INFN-LNF, Frascati, Italy
A. Cianchi, INFN and University of Rome "Tor Vergata", Rome, Italy
A. Mostacci, Dip. Energetica University of Rome "La Sapienza", Rome, Italy
C. Ronsivalle, ENEA C.R. Frascati, Italy

Abstract

A reliable transverse emittance measurement for high-brightness electron beams, in particular where the beam exhibits a significant energy spread, is of utmost importance for the successful development of the SPARC FEL. The effect of the emittance degradation induced by chromatic effects in the quadrupole scan measurement for different configurations of the magnetic lattice is evaluated. Analytical and numerical calculations compared with measurements are reported and discussed.

INTRODUCTION

The high energy transverse emittance measurement at SPARC is performed by means of a quadrupole scan [1] downstream the third accelerating section. The transverse beam size is measured on the flag F_1, which holds a YAG screen, for different values of current in quadrupoles Q_T1, Q_T2, Q_T3 (see Fig. 1). Single and multi-quadrupoles scan can be performed. A detailed study of different effects
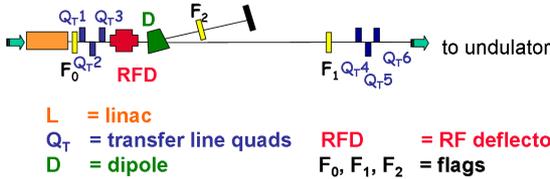
Figure 1: Layout of the high-energy experimental area.

affecting the emittance measurement with the quadrupole scan technique has been done for different lattice configurations, e.g. one and two quadrupoles and, in the latter setup, also with reversed currents.

The main advantage in using two quadrupoles with respect to the single quadrupole configuration is the possibility to measure both planes simultaneously. Moreover with two quadrupoles there is a better control of the beam shape, avoiding losses due to cut of beam tails. However, in order to observe a waist in both planes, the range of currents considered is wider and the focusing strength is stronger, thus the beam undergoes a stronger focalization [2].

The emittance degradation induced by chromatic effects in quadrupoles [3], [4] may represent a severe limitation of the quadrupole scan technique. At SPARC after beam compression via velocity bunching (VB) [5], the beam energy spread is of the order of 1% and, together with a large

transverse beam size at the entrance of the quadrupole, it might give a non negligible emittance growth. The evaluation of such emittance growth due to the aforementioned issues is object of the paper.

METHOD OF MEASUREMENT

With a well-centered beam, on the quadrupole magnetic axis, the rms beam size is measured as a function of the quadrupole field strength and the measurement described by the following matrix equation

$$
\begin{pmatrix} \sigma_1^2 \\ \sigma_2^2 \\ \vdots \\ \sigma_N^2 \end{pmatrix} = \begin{pmatrix} A_1^2 & 2A_1B_1 & B_1^2 \\ A_2^2 & 2A_2B_2 & B_2^2 \\ \vdots & \vdots & \vdots \\ A_N^2 & 2A_NB_N & B_N^2 \end{pmatrix} \begin{pmatrix} \beta\varepsilon \\ -\alpha\varepsilon \\ \gamma\varepsilon \end{pmatrix} \quad (1)
$$

where σ_j is the rms beam size measured at flag F_1 for the jth value of current, A_j and B_j the 11-element and 12-element of the 2x2 transport matrix of the lattice defined by three thick quadrupoles and a drift (see Fig. 1). The transverse emittance is determined by evaluating the Twiss parameters β, α and γ, resulting in the minimum χ^2 where [1], [6]

$$
\chi^2 = \sum_{j=1}^{N} \left[\frac{A_j^2\beta\varepsilon - 2A_jB_j\alpha\varepsilon + B_j^2\gamma\varepsilon - \sigma_j^2}{2\sigma_j u(\sigma_j)} \right]^2 \quad (2)
$$

with $u(\sigma_j)$ the uncertainty of the measurement. In order to compute the Twiss parameters at a given position (in our case the flag upstream Q_T1, i.e. F_0), the derivative of Eq. 2 with respect to $\beta\varepsilon$, $\alpha\varepsilon$, $\gamma\varepsilon$ has been done and the following system solved $\frac{\partial\chi^2}{\partial(\alpha\varepsilon)} = 0$, $\frac{\partial\chi^2}{\partial(\beta\varepsilon)} = 0$, $\frac{\partial\chi^2}{\partial(\gamma\varepsilon)} = 0$. Once the optimum Twiss parameters are found, the fitted rms beam sizes at the measurement flag F_1 are computed from Eq. 2 and compared to the measured data (Fig. 2). If the fit has a unique solution the lines enclose only one ellipse, i.e. a set of $\beta\varepsilon$, $\alpha\varepsilon$, $\gamma\varepsilon$ (see Fig. 4a and 4b).

The consistency of the χ^2-fit has been validated by means of a Trace3D virtual quadrupole scan, where the transverse beam size evolution as a function of the quadrupole current has been computed starting from measured emittance and Twiss parameters. As further validation of the SPARC high energy emittance measurement tool, the rms transverse beam sizes retrieved by Trace3D have been given as input to the emittance analysis program exhibiting an agreement within 2%.

* enrica.chiadroni@lnf.infn.it
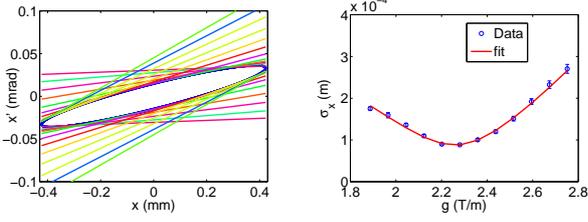
Figure 2: Left: retrieved ellipse in the trace space enclosed by tangent lines corresponding to the set of measurements. Right: measured horizontal rms beam size (blue dots) compared to the χ^2-fit (red curve) as function of quadrupole gradient (two quadrupoles configuration; 300 pC, 147 MeV).

LIMITATIONS TO QSCAN TECHNIQUE

In quadrupole scan measurements a monochromatic electron beam is assumed to evaluate the projected emittance. However, for a real beam, particles have an energy spread different from zero. The validity of this assumption is matter of discussion.

Let us call ε_1 the emittance after the quadrupole, with k and ℓ its gradient and length, respectively. Let σ_γ be the beam energy spread, and σ_x and emittance ε_0 the rms size and emittance at the quadrupole entrance. Starting from the statistical definition of emittance, in case of single quadrupole (in thin lens approximation) and only assuming the particle energy uncorrelated from its transverse position, one gets

$$\varepsilon_1^2 = \varepsilon_0^2 + (k\ell)^2 \sigma_x^4 \sigma_\gamma^2 = \varepsilon_0^2 + \varepsilon_c^2, \qquad (3)$$

that is

$$\varepsilon_1 = \varepsilon_0 + \Delta\varepsilon \quad \text{with} \quad \Delta\varepsilon = -\varepsilon_0 + \sqrt{\varepsilon_0^2 + \varepsilon_c^2}$$

and in case of $\varepsilon_0 \ll \varepsilon_c$

$$\frac{\Delta\varepsilon}{\varepsilon_0} \simeq \frac{\varepsilon_c}{\varepsilon_0} - 1 + \frac{\varepsilon_0}{2\varepsilon_c} \simeq \frac{\varepsilon_c}{\varepsilon_0}. \qquad (4)$$

On the contrary, in the limit of $\varepsilon_0 \gg \varepsilon_c$

$$\frac{\Delta\varepsilon}{\varepsilon_0} \simeq \frac{\varepsilon_c^2}{2\varepsilon_0^2}, \qquad (5)$$

as given in [4] to account for the chromatic dependence of emittance.

In case of high brightness electron beams, since the emittance approaches 1 mm-mrad, the product $\sigma_x^2 \sigma_\gamma$ might be large with respect to ε_0, thus the emittance growth due to chromatic effects in a single quadrupole follows the dependence found in Eq. 4.

In case of two quadrupoles at a distance L, and strength depending on the particle energy, so that $(k_i \ell_i)(1-\delta) = K_i(1-\delta)$ for $i = 1, 2$, with $K_i = k_i \ell_i$, Eq. 4 becomes

$$
\begin{aligned}
\varepsilon_1^2 =\ & \varepsilon_0^2 + f(K_1, K_2, L)\sigma_\gamma^2\sigma_x^4 + g(K_1, K_2, L)\sigma_\gamma^2\sigma_{x'}^4 + \\
& h(K_1, K_2, L)\sigma_\gamma^2\sigma_{xx'}^2 + t(K_1, K_2, L)\sigma_\gamma^2\sigma_x^2\sigma_{x'}^2 + \\
& u(K_1, K_2, L)\sigma_\gamma^2\sigma_x^2\sigma_{xx'} + \\
& v(K_1, K_2, L)\sigma_\gamma^2\sigma_{x'}^2\sigma_{xx'},
\end{aligned}
\qquad (6)
$$

where $\sigma_\gamma^2 = \langle \delta^2 \rangle$, $\sigma_x^2 = \langle x_0^2 \rangle$, $\sigma_{x'}^2 = \langle x_0'^2 \rangle$, $\sigma_{xx'} = \langle x_0 x_0' \rangle$,

$$
\begin{aligned}
f(K_1, K_2, L) &= \{K_2 + K_1[1 + K_2L(-2 + K_1L)]\}^2 \\
g(K_1, K_2, L) &= L^4 K_2^2 \\
h(K_1, K_2, L) &= 4L(1 - K_1L)(2K_1K_2L + \\
& \quad K_2^2 L - 3K_1K_2^2 L^2) \\
t(K_1, K_2, L) &= 2K_2(K_2 - K_1)L^2 - 4K_1K_2^2L^3 + \\
& \quad 2K_1^2K_2^2L^4 \\
u(K_1, K_2, L) &= 4K_2L(1 - K_1L)\{K_2 + \\
& \quad K_1[1 - K_2L(2 - K_1L)]\} \\
v(K_1, K_2, L) &= 4K_2^2L^3(1 - K_1L).
\end{aligned}
$$

In what follows, we explore the contribution to the emittance for practical cases encountered at SPARC.

For this study the SPARC high energy emittance measurement tool has been used, together with both a virtual quadrupole scan code, to create the evolution of the transverse beam size, and the macro-particle TSTEP code in order to investigate all the effects which may affect the high energy emittance measurement.

Three virtual measurements, keeping the beam charge constant (300 pC), have been done in three different beam configurations summarized in table 1. For each config-

Table 1: Virtual measurement parameters.

	On crest beam[1]	Compressed beam with solenoids OFF[2]	Compressed beam with solenoids ON[3]
σ_{x,F_0} (mm)	0.571	1.735	0.343
σ_{y,F_0} (mm)	0.595	1.788	0.341
σ_γ (%)	0.169	0.993	0.959

uration, different magnetic lattices for the quadrupole scan have been explored, i.e. single quadrupole for both horizontal and vertical planes, two quadrupoles with first focusing (Q_T1) and second defocusing (Q_T3) in horizontal plane, and *viceversa*.

Table 2 summarizes the results obtained from the virtual measurement for the uncompressed beam, corresponding to small energy spread (< 2). The reference values are computed at the flag F_0 by means of a simulation with TSTEP code. In the single quadrupole scan measurement the agreement with reference values is within 0.4%, while in the two-quadrupoles scan the agreement is still satisfactory, and within 0.5%, only in the plane in which Q_T1 is focusing (i.e. horizontal in "+ -" configuration and vertical in the "- +" one), the emittance being overestimated otherwise.

Results for the horizontal and vertical emittance in case of large energy spread and large spot size at the quadrupole

---

[1]Not compressed beam: low energy spread, $\sigma_\gamma \approx 1$.

[2]VB operation and solenoids off on first two traveling wave (TW) linac sections: high $\sigma_\gamma \approx 1\%$ and large $\sigma_{x,y,F_0} \approx$ mm.

[3]VB operation and solenoids powered on first two TW linac sections: high $\sigma_\gamma \approx 1\%$ and small $\sigma_{x,y,F_0} \approx 10^2 \mu$m.

Table 2: Not compressed beam.

	Reference value	Single quad	Two quads (+, -)	Two quads (-, +)
$\varepsilon_{n,x}$ (mm mrad)	1.375	1.372	1.380	1.535
$\varepsilon_{n,y}$ (mm mrad)	1.413	1.419	1.590	1.420
σ_γ (%)	0.169			

entrance are shown in Table 3. A strong disagreement,

Table 3: Compressed beam and solenoids OFF.

	Reference value	Single quad	Two quads (+, -)	Two quads (-, +)
$\varepsilon_{n,x}$ (mm mrad)	3.07	4.32	4.78	8.76
$\varepsilon_{n,y}$ (mm mrad)	3.02	4.38	9.07	4.87
σ_γ (%)	0.993			

of the order of 30% in both planes, is evident in the single quadrupole, while in the two-quadrupoles configuration the disagreement is within 40% only in the plane where the first quadrupole is focusing. It increases dramatically up to 200% otherwise.

In order to highlight quadrupoles chromatic effects, the output projected emittance is plotted as function of quadrupole current for both single quadrupole (Fig. 3a) and two-quadrupoles (Fig. 3b) configuration in case of compressed beam with TW solenoids off. Lower energy parti-

(a) (b)
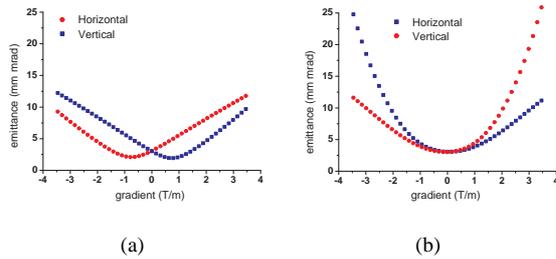
Figure 3: Output emittance in case of both large σ_γ and spot size as function of the quadrupole gradient for single (a) and two-quadrupole (b) configuration.

cles get a larger kick with respect to higher energy ones. The emittance growth depends then on the quadrupole strength and with two quadrupoles the effect is stronger and more asymmetric than with a single quadrupole due to the fact that the range of currents is wider and the focusing strength stronger in the former case. The partial compensation of emittance, visible in Fig. 3 and Fig. 5 for quadrupole currents smaller than 1 A, with respect to the case with quadrupoles set at zero current can be explained

with the non-null correlations between transverse coordinates and energy in the beam exiting from the linac.

In order to evaluate the influence of chromatic effects, a monochromatic electron beam has been assumed in the virtual measurement. As expected, the emittance growth induced by chromatic effects is canceled in both single and two quadrupoles scan with an agreement of about 2% (see Table 4). However even in the assumption of a monochro-

Table 4: Compressed monochromatic beam and solenoids OFF.

	Reference value	Single quad	Two quads (+, -)	Two quads (-, +)
$\varepsilon_{n,x}$ (mm mrad)	3.07	3.02	3.011/2.95[1]	3.097/4.86[1]
$\varepsilon_{n,y}$ (mm mrad)	3.02	2.974	3.08/5.02[1]	2.97/2.88[1]
σ_γ(%)	0			

matic beam some asymmetries and errors might still be evident in the two quadrupoles measurement if a too large current step is used (see Table 4, results labeled as 1). The reason of the residual error and asymmetry appears in plots of Fig. 4a and Fig. 4b showing the graphical output of the quadrupole scan measurement tool for the two steps considered. Despite the fitting curve well reproduces data, with a step of 0.2 A the identification of the minimum is poor, resulting in an asymmetry of the retrieved emittance values. Table 5 summarizes results for the case of high

(a)

(b)
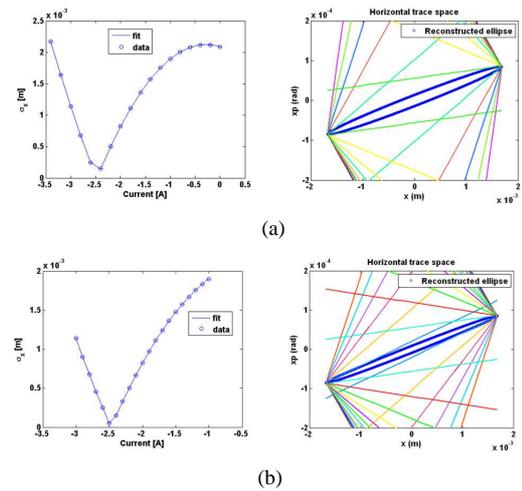
Figure 4: Result of the two-quadrupoles scan ("+ -") corresponding to emittance values listed in Table 4: (a) amounts to a poor and (b) to a satisfactory sampling of the waist. Despite the fitting curve well reproduces the data, the ellipse is uniquely defined only in (b).

energy spread and small spot size at flag F_0, due to the additional focusing provided by solenoids around the first two linac sections. Despite of the large energy spread a

---

[1]The current step is 0.2 A, while 0.1 A otherwise.

Table 5: Compressed beam and solenoids ON.

	Reference value	Single quad	Two quads (+, -)	Two quads (-, +)
$\varepsilon_{n,x}$ (mm mrad)	1.483	1.483	1.476	1.540
$\varepsilon_{n,y}$ (mm mrad)	1.495	1.490	1.555	1.491
$\sigma_\gamma(\%)$	0.959			

very good agreement with the single quadrupole measurement is shown. A better agreement is also evident with two quadrupoles with respect to the virtual measurement with no solenoids, even though a small asymmetry is still visible in the two planes (see Fig. 5).

(a)   (b)
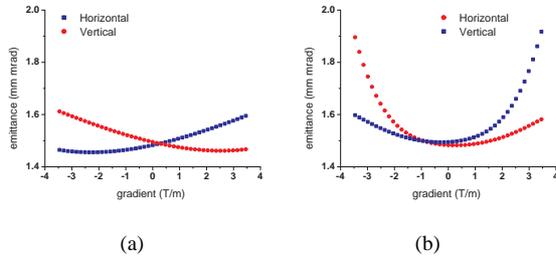
Figure 5: Output emittance in case of large energy spread but small spot size as function of the quadrupole gradient for single (a) and two-quadrupoles (b) configuration.

Measurements

In order to investigate the disagreement shown by virtual measurements between single and multi quadrupoles measurement in different quadrupole configurations, some measurements have been performed in case of uncompressed beam, i.e. low energy spread of the order of 0.1%, and modest transverse beam size at F_0. Results are summarized in Table 6. The measured emittance values

Table 6: Uncompressed beam.

	Single quad	Two quads (+, -)[1]	Two quads (-, +)[2]
σ_{x,F_0}(mm)	0.29	0.32	0.35
σ_{y,F_0}(mm)	0.37	0.35	0.35
$\varepsilon_{n,x}$(mm mrad)	1.60	1.84	2.40
$\varepsilon_{n,y}$(mm mrad)	1.40	2.36	1.72

for the two quadrupoles configuration are systematically higher than those measured in single quadrupole one. Furthermore they show the same asymmetry highlighted by simulations, i.e. the emittance results higher in the plane where the first quadrupole is defocusing. This means that also for uncompressed beams second order effects might affect the measurement.

---

[1] $Q_T 1$ is focusing and $Q_T 3$ defocusing in horizontal plane.
[2] $Q_T 1$ is focusing and $Q_T 3$ defocusing in vertical plane.

Eventually, Fig. 6 shows the results of a measurement in which the effect discussed above resulted particularly evident: it concerns the measurement of the horizontal emittance on a 0.86% energy spread beam with a rms spot size in F_0 of 1.4 mm compressed in the SPARC linac via the VB technique, but with the emittance compensation solenoid off on the TW sections. Due to the combined effect of
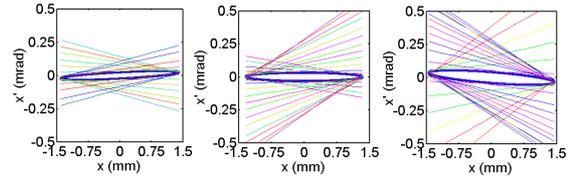
Figure 6: Horizontal trace space for a 0.86% energy spread, σ_{x,F_0}=1.4 mm beam: single quadrupole (left) and two quadrupoles ("+ -" (center) and "- +" (right).

large energy spread and spot size, we observed a strong difference in the horizontal emittance measurement with one quadrupole (7.00 ± 0.34 mm-mrad), two quadrupoles in "+ -" (8.64 ± 0.23 mm-mrad) and in "+ -" setting (12.25 ± 0.45 mm-mrad), and also in the Twiss parameters.

CONCLUSIONS

The theoretical and experimental comparison between one quadrupole and two quadrupoles scan emittance measurement has shown that, despite some practical advantages, the two quads scan measurement can introduce some errors in the emittance evaluation. In particular the chromatic effects are enhanced and can affect the measurement sensitively especially for large spot sizes. In addition some asymmetries can be induced also for low energy spread beams if in the measurement the minimum spot size is not defined with sufficient accuracy in both planes during the quadrupoles current variation.

Further measurements are foreseen to identify the threshold of the product between beam size and energy spread, which produces significant chromatic effects in the projected emittance measurement, and to evaluate the chromatic effects in case of misalignment of quadrupoles.

REFERENCES

[1] M. Minty and F. Zimmermann, "Measurement and control of charged particle beams", Springer (2003) p. 99.

[2] E. Chiadroni et al., Conf. Proc. DIPAC09, (2009).

[3] X.J. Wang et al., "Experimental results of the ATF in-line injection system", Conf. Proc. PAC95, p.890.

[4] J. Buon, "Beam Phase Space and Emittance", CERN 94-01, vol. I, p. 89.

[5] M. Ferrario et al., Phys. Rev. Lett. **104**, 054801 (2010).

[6] H. Braun, "Emittance Diagnostics I, II", CERN School on Beam Diagnostics, Dourdan, France (2008).